

See discussions, stats, and author profiles for this publication at: <https://www.researchgate.net/publication/6938267>

Interfacial Synthesis of Dendritic Platinum Nanoshells Templated on Benzene Nanodroplets Stabilized in Water by a Photocatalytic Lipoporphyrin

ARTICLE *in* JOURNAL OF THE AMERICAN CHEMICAL SOCIETY · AUGUST 2006

Impact Factor: 12.11 · DOI: 10.1021/ja0619859 · Source: PubMed

CITATIONS

46

READS

33

4 AUTHORS, INCLUDING:



[Yujiang Song](#)

Dalian University of Technology

57 PUBLICATIONS 1,310 CITATIONS

[SEE PROFILE](#)



[Craig Medforth](#)

University of Porto

167 PUBLICATIONS 5,966 CITATIONS

[SEE PROFILE](#)



[John A Shelnutt](#)

University of Georgia

265 PUBLICATIONS 8,722 CITATIONS

[SEE PROFILE](#)

Donor–Acceptor Biomorphs from the Ionic Self-Assembly of Porphyrins

Kathleen E. Martin,[†] Zhongchun Wang,[†] Tito Busani,[‡] Robert M. Garcia,[†] Zhu Chen,[†] Yingbing Jiang,^{†,§} Yujiang Song,[†] John L. Jacobsen,^{||} Tony T. Vu,^{||} Neil E. Schore,^{||} Brian S. Swartzentruber,[†] Craig J. Medforth,^{†,§,||} and John A. Shelnutt^{*,†,⊥}

Advanced Materials Laboratory and Center for Integrated Nano Technologies, Sandia National Laboratories, Albuquerque, New Mexico 87185-1349, Universidade Nova de Lisboa at CENIMAT/I3N, Departamento de Ciéncia dos Materiais, Faculdade de Ciéncias e Tecnologia, FCT, Universidade Nova de Lisboa and CEMOP-UNINOVA, 2829-516 Caparica, Portugal, Department of Chemical & Nuclear Engineering, University of New Mexico, Albuquerque, New Mexico 87106, Department of Chemistry, University of California, Davis, California 95616, and Department of Chemistry, University of Georgia, Athens, Georgia 30602

Received March 15, 2010; E-mail: jasheln@unm.edu

Abstract: Microscale four-leaf clover-shaped structures are formed by self-assembly of anionic and cationic porphyrins. Depending on the metal complexed in the porphyrin macrocycle (Zn or Sn), the porphyrin cores are either electron donors or electron acceptors. All four combinations of these two metals in cationic tetra(N-ethanol-4-pyridinium)porphyrin and anionic tetra(sulfonatophenyl)porphyrin result in related cloverlike structures with similar crystalline packing indicated by X-ray diffraction patterns. The clover morphology transforms as the ionic strength and temperature of the self-assembly reaction are increased, but the structures maintain 4-fold symmetry. The ability to alter the electronic and photophysical properties of these solids (e.g., by altering the metals in the porphyrins) and to vary cooperative interactions between the porphyrin subunits raises the possibility of producing binary solids with tunable functionality. For example, we show that the clovers derived from anionic Zn porphyrins (electron donors) and cationic Sn porphyrins (electron acceptors) are photoconductors, but when the metals are reversed in the two porphyrins, the resulting clovers are insulators.

Introduction

Nanostructures self-assembled from organic molecules are of great interest because of their potential applications in areas such as organic solar cells and electronics, sensors, and catalysis.^{1–8} In particular, these organic nanostructures offer new opportunities for mimicking the processes that occur in biological photosynthesis to produce fuels or to produce electrical energy in organic solar cells, and this possibility is especially

true when the subunits of these nanostructures are the chlorophyll-related porphyrins.^{9–23} In fact, molecules of bacteriochlorophyll—a porphyrin derivative—assemble to form the nanorods in the chlorosomes of green bacteria, and these chlorosomal rods are

- [†] Sandia National Laboratories.
[‡] Universidade Nova de Lisboa at CENIMAT/I3N.
[§] University of New Mexico.
^{||} University of California.
[⊥] University of Georgia.
- (1) Chen, Z. P.; Debije, M. G.; Debaerdemaeker, T.; Osswald, P.; Würthner, F. *ChemPhysChem* **2004**, 5, 137.
(2) Jones, B. A.; Ahrens, M. J.; Yoon, M.-H.; Facchetti, A.; Marks, T. J.; Wasielewski, M. R. *Angew. Chem., Int. Ed.* **2004**, 43, 6363.
(3) An, Z.; Yu, J.; Jones, S. C.; Barlow, S.; Yoo, S.; Domercq, B.; Prins, P.; Siebbeles, L. D. A.; Kippelen, B.; Marder, S. R. *Adv. Mater.* **2005**, 17, 2580.
(4) Shin, W. S.; Jeong, H.-H.; Kim, M.-K.; Jin, S.-H.; Kim, M.-R.; Lee, J.-K.; Lee, J. W.; Gal, Y.-S. *J. Mater. Chem.* **2006**, 16, 384.
(5) An, Z.; Odom, S. A.; Kelley, R. F.; Huang, C.; Zhang, X.; Barlow, S.; Padilha, L. A.; Fu, J.; Hagan, D. J.; Van Stryland, E. W.; Wasielewski, M. R.; Marder, S. R. *J. Phys. Chem. A* **2009**, 113, 5585.
(6) Cui, S.; Liu, H.; Gan, L.; Li, Y.; Zhu, D. *Adv. Mater.* **2008**, 20, 2918.
(7) Zhou, W. D.; Li, Y. L.; Zhu, D. B. *Chem. Asian J.* **2007**, 2, 222.
(8) Gan, H.; Liu, H.; Li, Y.; Zhao, Q.; Li, Y.; Wang, S.; Jiu, T.; Wang, N.; He, X.; Yu, D.; Zhu, D. *J. Am. Chem. Soc.* **2005**, 127, 12452.
- (9) Wang, Z.; Ho, K. J.; Medforth, C. J.; Shelnutt, J. A. *Adv. Mater.* **2006**, 18, 2557.
(10) Wang, Z.; Li, Z.; Medforth, C. J.; Shelnutt, J. A. *J. Am. Chem. Soc.* **2007**, 129, 2440.
(11) Wang, Z.; Lybarger, L. E.; Wang, W.; Medforth, C. J.; Miller, J. E.; Shelnutt, J. A. *Nanotechnology* **2008**, 19, 395604.
(12) Wang, Z.; Medforth, C. J.; Shelnutt, J. A. *J. Am. Chem. Soc.* **2004**, 126, 16720.
(13) Wang, Z.; Medforth, C. J.; Shelnutt, J. A. *J. Am. Chem. Soc.* **2004**, 126, 15954.
(14) Vlaming, S. M.; Augulis, R.; Stuart, M. C. A.; Knoester, J.; van Loosdrecht, P. H. M. *J. Phys. Chem. B* **2009**, 113, 2273.
(15) Schwab, A. D.; Smith, D. E.; Bond-Watts, B.; Johnston, D. E.; Hone, J.; Johnson, A. T.; de Paula, J. C.; Smith, W. F. *Nano Lett.* **2004**, 4, 1261.
(16) Sandanayaka, A. S. D.; Araki, Y.; Wada, T.; Hasobe, T. *J. Phys. Chem. C* **2008**, 112, 19209.
(17) Rosaria, L.; D'Urso, A.; Mammana, A.; Purrello, R. *Chirality* **2008**, 20, 411.
(18) Purrello, R. *Nat. Mater.* **2003**, 2, 216.
(19) Lee, S. J.; Hupp, J. T.; Nguyen, S. T. *J. Am. Chem. Soc.* **2008**, 130, 9632.
(20) Karan, S.; Mallik, B. *J. Phys. Chem. C* **2008**, 112, 2436.
(21) Drain, C. M.; Varotto, A.; Radivojevic, I. *Chem. Rev.* **2009**, 109, 1630.
(22) Drain, C. M. *Proc. Natl. Acad. Sci. U.S.A.* **2002**, 99, 5178.
(23) Bard, A. J.; Fox, M. A. *Acc. Chem. Res.* **1995**, 28, 141.

the largest and most efficient harvesters of light known.^{24–29} It is of interest to examine the possibility of producing similar self-assembled porphyrin-based structures from synthetic porphyrins for the purpose of generating efficient light-harvesting components of artificial photosynthetic systems, dye-sensitized solar cells, and organic photovoltaics.

We and others have been exploring the self-assembly of porphyrin nanostructures by various methods including reprecipitation, coordination polymerization, surfactant-induced self-assembly, and ionic self-assembly.^{9–23,30–32} Ionic self-assembly³³ is particularly interesting; while the properties of these binary porphyrin nanomaterials are relatively unknown, they potentially offer unique and tunable characteristics that result from the cooperative interactions between the two types of porphyrin cores in the solid. Herein, we describe some extraordinary microscale-sized porphyrin biomorphs (nonbiological structures that are shaped like living organisms) obtained by the self-assembly of two oppositely charged porphyrin ions (tectons). For the Zn(II) and Sn(IV) complexes investigated, the overall shape, size, and crystalline structures of these biomorphs are largely independent of which metals are in the two porphyrins. However, the metal-centered interactions play a dominant role in determining the electronic characteristics of the porphyrin macrocycles (e.g., electron donor versus electron acceptor). This combination of factors potentially allows a high degree of control over the cooperative interactions between the porphyrin cores (e.g., charge transfer) and consequently the functionality (e.g., charge separation and migration) of the organic solid. We expect that these new materials will have applications in solar energy technologies and organic electronics and optoelectronics.

Materials and Methods

Synthesis of Clovers. Zn^{II}TPPS⁴⁻ and Sn^{IV}TPPS⁴⁻ were obtained from Frontier Scientific. Sn^{IV}T(N-EtOH-4-Py)P⁴⁺ was purchased from Ambinter. Zn^{II}T(N-EtOH-4-Py)P⁴⁺ was prepared by dissolving H₂T(N-EtOH-4-Py)P⁴⁺ (58 mg) (Frontier Scientific) in methanol (5 mL), adding Zn(OAc)₂ (29 mg), and stirring the solution for 1 h. Chloroform (90 mL) was then added, and a stream of air was passed over the solution until a green film developed on the surface. The film was removed using a pipet and dried under vacuum for 24 h. The purity of the porphyrins was confirmed by proton NMR spectroscopy of D₂O solutions of the materials. Stock solutions of the porphyrins (210 μM) were prepared in NANOpure water and used in the self-assembly reactions. In a typical self-assembly reaction, 10 mL aliquots of stock solutions were added to a 20 mL glass vial, mixed by shaking for 30 s, and left undisturbed and shielded from light for 2 days. The clovers were obtained as a dark green precipitate at the bottom of the glass vial.

- (24) Saga, Y.; Tamiaki, H. *J. Biosci. Bioeng.* **2006**, *102*, 118.
- (25) Ganapathy, S.; Oostergetel, G. T.; Wawrzyniak, P. K.; Reus, M.; Chew, A. G. M.; Buda, F.; Boekema, E. J.; Bryant, D. A.; Holzwarth, A. R.; de Groot, H. J. M. *Proc. Natl. Acad. Sci. U.S.A.* **2009**, *106*, 8525.
- (26) Cohen-Bazire, G.; Pfennig, N.; Kunisawa, R. *J. Cell Biol.* **1964**, *22*, 207.
- (27) Holt, S. C.; Conti, S. F.; Fuller, R. C. *J. Bacteriol.* **1966**, *91*, 311.
- (28) Pierson, B. K.; Castenholz, R. W. In *The Photosynthetic Bacteria*; Clayton, R. K., Sistrom, W. R., Eds.; Plenum Publishing Corp.: New York, 1978; p 179.
- (29) Sprague, S. G.; Staehelin, A. L.; DiBartolomeis, M. J.; Fuller, R. C. *J. Bacteriol.* **1981**, *147*, 1021.
- (30) Medforth, C. J.; Wang, Z.; Martin, K. E.; Song, Y.; Jacobsen, J. L.; Shelton, J. A. *Chem. Commun.* **2009**, 7261.
- (31) Lee, S. J.; Jensen, R. A.; Malliakas, C. D.; Kanatzidis, M. G.; Hupp, J. T.; Nguyen, S. T. *J. Mater. Chem.* **2008**, *18*, 3640.
- (32) Lee, S. J.; Malliakas, C. D.; Kanatzidis, M. G.; Hupp, J. T.; Nguyen, S. T. *Adv. Mater.* **2008**, *20*, 3543.
- (33) Faul, C. F. J.; Antonietti, M. *Adv. Mater.* **2003**, *15*, 673.

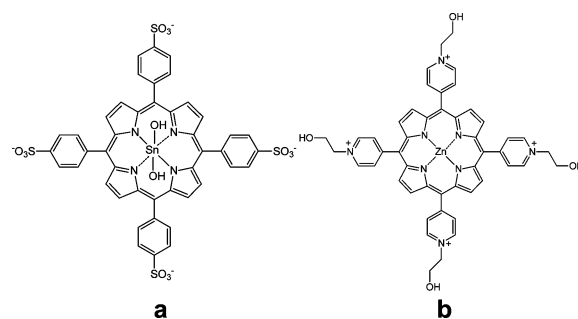


Figure 1. Structures of (a) tin(IV) tetrakis(4-sulfonatophenyl)porphyrin (SnTPPS⁴⁻) and (b) zinc(II) tetrakis(N-ethanol-4-pyridinium)porphyrin [ZnT(N-EtOH-4-Py)P⁴⁺].

Clover Characterization. The composition of the clovers was determined by calculating the amount of each porphyrin removed from solution and incorporated into the product. Optical absorption spectra of the supernatants were measured after centrifugation to remove the precipitated product, and porphyrin concentrations were calculated from extinction coefficients measured using diluted stock solutions of the porphyrin monomers.

Samples for imaging were prepared by pipetting 50 μL of the precipitate layer onto Si wafers (scanning electron microscopy, SEM) or p-type Si wafers (atomic force microscopy, AFM). Excess solvent was wicked away after 10 min using a Kimwipe tissue, and the wafer was air-dried. SEM imaging was performed on a Hitachi S-5200 Nano Scanning Electron Microscope operating at 1–2 keV. AFM measurements were carried out on a Nanoscope III Multimode AFM (Digital Instruments, United States) in contact mode using Si cantilevers.

Samples for X-ray diffraction (XRD) measurements were prepared either by depositing the powder (dried by mild heating) onto glass slides (VWR) or Si wafers or by depositing a drop of a suspension of the clovers onto the glass slide and allowing it to dry in air. XRD spectra were recorded on a Siemens D500 diffractometer using Ni-filtered Cu Kα radiation with $\lambda = 1.5418 \text{ \AA}$ in θ –2 θ scan mode using a step size of 0.05° and a 90 s step time.

Salt-, Temperature-, and Time-Dependent Studies. The self-assembly reaction of ZnT(N-EtOH-4-Py)P⁴⁺ and SnTPPS⁴⁻ was repeated using modified versions of the procedure described above. All reactions were carried out by mixing 1 mL aliquots in a 4 mL glass vial. For the salt-dependent studies, sodium chloride (99+, Aldrich) was added to the 210 μM porphyrin stock solutions to produce salt concentrations of 1, 2, 5, 10, 15, or 20 mM. The saline stock solutions were then added to a 4 mL glass vial, mixed by shaking for 30 s, and left undisturbed and shielded from light for 24 h. For the temperature-dependent studies, 1 mL aliquots were equilibrated at the required temperature (10, 23, 60, or 80 °C) for 1 h, rapidly mixed, and then returned to the temperature-controlled environment for 24 (10 or 23 °C) or 4 h (60 or 80 °C). In the time-dependent study, aliquots of the stock solutions were mixed by shaking the vial for 5 s, and 50 μL portions were removed and placed onto Si wafers after 0.5, 5, 10, 20, 30, 60, and 120 min. The excess liquid was immediately wicked away, the wafer was washed with 2 drops of NANOpure water, excess liquid was again removed, and the wafer was allowed to air dry.

Results and Discussion

Zinc(II) or tin(IV) was chosen as the metal for the porphyrins, as these give electron donor or acceptor porphyrin macrocycles, respectively (see below). Self-assembly of SnTPPS⁴⁻ and ZnT(N-EtOH-4-Py)P⁴⁺ (Figure 1) produced a dark green precipitate. SEM images of the material (Figure 2) reveal remarkable “four-leaf clover”-like structures. The clovers are approximately square with average edge lengths ranging from

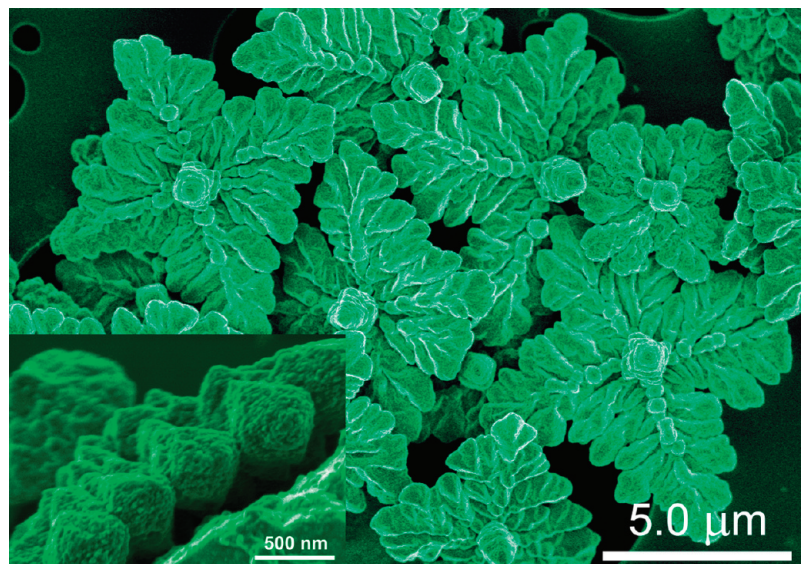


Figure 2. Low magnification SEM image of the Sn/Zn porphyrin clovers. Inset: High magnification image of a clover in an edge-on orientation.

2.0 to 10.0 μm (as determined by measuring randomly selected clovers from several images and preparations). The clovers are a few hundred nanometers thick, as determined from SEM images of clovers trapped edge on to the electron beam (see Figure 2, inset). Four leaves with well-defined “veins” (especially the midrib vein) are readily apparent, as well as a central “stem” or “stalk”. Complex nanoscale features are visible in high magnification images shown in the inset of Figure 2 and in Figure S1 of the Supporting Information.

The formation of inorganic biomorphic structures during the bottom-up synthesis of nanomaterials is well-known in the literature.³⁴ However, this is probably the most striking example of a porphyrin-related biomorph. The most closely related biomorphic structure previously observed is the nanoflower obtained by vapor deposition of a phthalocyanine.²⁰ There have been no previously reported biomorphs composed of a binary porphyrin solid like those described here.

Analysis of the UV-visible spectra of the supernatant remaining after the synthesis of the clovers using equimolar porphyrin concentrations shows that greater than 95% of each porphyrin present initially has reacted. This indicates a 1:1 ratio of the porphyrin ions in the product and is expected¹³ for an ionic solid obtained from the self-assembly of porphyrin ions that have equal but opposite charges. There is also no evidence from EDX that significant amounts of small counterions (e.g., Na^+ or Cl^-) are present in the clovers.

Figure S2 of the Supporting Information shows SEM images of the clovers after different reaction times. The images show that the cloverlike morphology is already established after only 30 s, with nascent square clovers as large as 500 nm on an edge. In agreement with this result, cloudiness of the solution is observed immediately after mixing the porphyrin solutions. Mature clovers are observed after only 5 min. These findings suggest rapid growth by diffusion-limited aggregation from an initially supersaturated binary porphyrin solution (100 μM). Consistent with this interpretation, dissolution of the cloverlike dendrites in water produces very low ($<1 \mu\text{M}$) concentrations of SnTPPS^{4-} or $\text{ZnT(N-EtOH-4-Py)}\text{P}^{4+}$ monomers.

(34) Ruiz, J. M. G.; Carnerup, A.; Christy, A. G.; Welham, N. J.; Hyde, S. T. *Astrobiology* 2002, 2, 353.

SEM images in Figure 3 show that ionic strength (i.e., NaCl added to the reactant solutions) influences the morphology of the clovers. Specifically, a smooth four-pointed star shape is seen at the highest salt concentration (20 mM) in contrast to the complex four-leaf clover motif shown in Figure 2. The salt dependence of the morphology might be explained by a variation in the diffusion-limited rate of growth. Increasing the ionic strength shields the charged groups on the anionic and cationic porphyrins, likely slowing the ionic self-assembly process. We also note an increase in the diversity of morphologies obtained as the salt concentration increases (Figure S3 of the Supporting Information).

The temperature at which self-assembly takes place has an even more pronounced influence on morphology than the changes in ionic strength. Figure 4 shows SEM images of the structures obtained for growth at four temperatures between 10 and 80 °C. Notice that the structures retain the basic 4-fold symmetry of the clovers but have less pronounced nanoscale features as the growth temperature is increased, until at 80 °C the structures have transformed into a smooth and podlike shape. Just as for high ionic strength, high temperature might influence the diffusion-limited self-assembly of these dendritic structures, changing the morphology. Varying the growth temperature is also expected to change the solubility of the ionic solid, and this might also influence the diffusion-limited growth rate. Greater diversity is also seen in the structures obtained at high temperatures (Figure S4 of the Supporting Information), as was noted for structures obtained at increased ionic strength (see Figure S3 of the Supporting Information).

Microclovers of the same general shape and size are obtained by switching the metals in the two porphyrins (Figure 5b), that is, using ZnTPPS^{4-} and $\text{SnT(N-EtOH-4-Py)}\text{P}^{4+}$ to prepare Zn/Sn clovers. Moreover, cloverlike structures are even obtained when either both tectons are tin porphyrins (Sn/Sn clovers, Figure 5c) or both are zinc porphyrins (Zn/Zn clovers, Figure 5d). This is consistent with the interactions between the porphyrin ions being the dominant factor determining the structure. That is, intermolecular interactions arising from the metals (Zn, Sn) in the porphyrin play only a minor role, so that cloverlike structures are produced regardless of the metals contained in the porphyrins. Other six-coordinate metallopor-

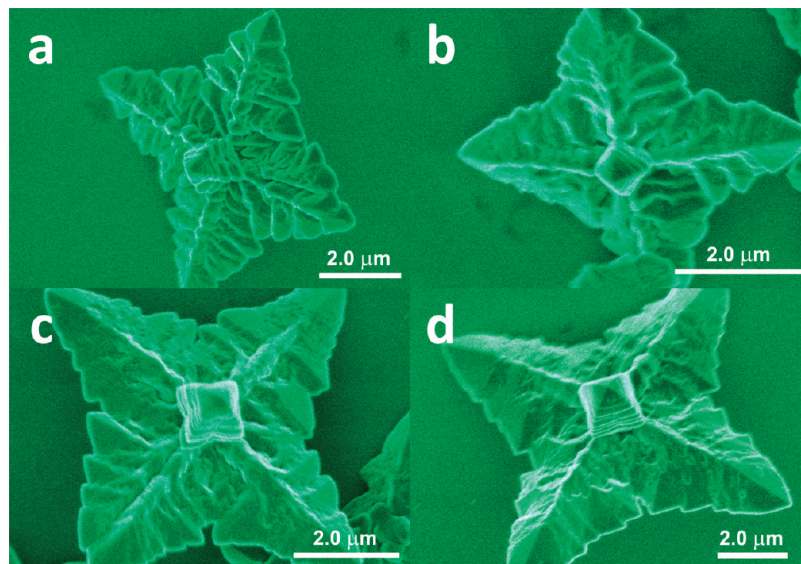


Figure 3. Growth of SnTPPS^{4-} and $\text{ZnT}(\text{N-EtOH-4-Py})\text{P}^{4+}$ clovers at 23 °C with differing concentrations of added NaCl . SEM images obtained for (a) 5, (b) 10, (c) 15, and (d) 20 mM added salt. Excess salt has been washed away for these images.

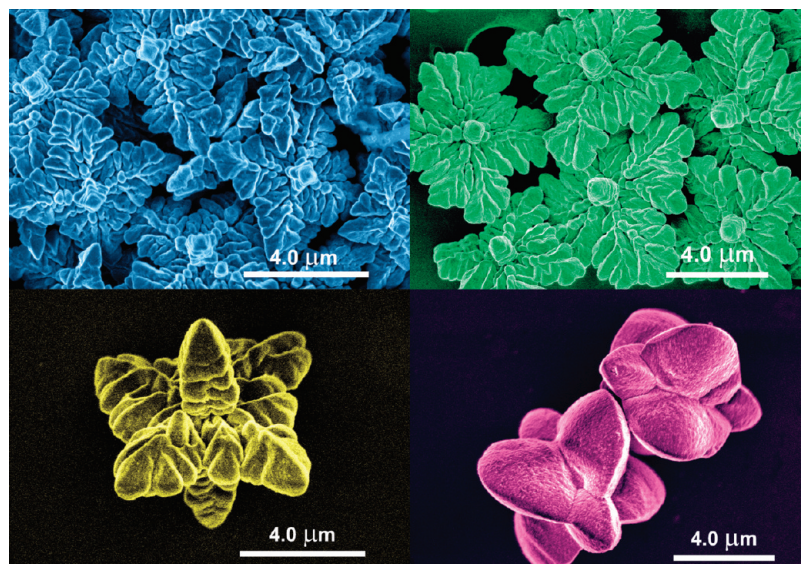


Figure 4. Growth temperature dependence of SnTPPS^{4-} and $\text{ZnT}(\text{N-EtOH-4-Py})\text{P}^{4+}$ structures. SEM images obtained for growth at 10 (blue), 23 (green), 60 (gold), and 80 °C (pink).

porphyrins can also be used to generate cloverlike structures. Ionic self-assembly of ZnTPPS^{4-} with $\text{Co(III)}\text{T}(\text{N-EtOH-4-Py})\text{P}^{4+}$ or $\text{Mn(III)}\text{TPPS}^{4-}$ with $\text{ZnT}(\text{N-EtOH-4-Py})\text{P}^{4+}$ (Figure S5 of the Supporting Information) both produce cloverlike structures. In contrast, ionic self-assembly reactions where one of the metalloporphyrins is four-coordinate [e.g., $\text{Ni(II)}\text{TPPS}^{4-}$ with $\text{ZnT}(\text{N-EtOH-4-Py})\text{P}^{4+}$ or $\text{Cu(II)}\text{TPPS}^{4-}$ with $\text{SnT}(\text{N-EtOH-4-Py})\text{P}^{4+}$] have not yielded clovers or other discrete nanostructures. Further studies are underway to determine the range of porphyrin metal complexes and axial ligands that produces clovers. In addition, we are investigating what other morphologies can be obtained with different combinations of porphyrin ions and coordinated metals.

The most obvious difference among the structures obtained with the Zn and Sn complexes of TPPS and T(N-EtOH-4-Py)P is that only clovers obtained with SnTPPS^{4-} (Figure 5a,c) have pronounced central stems. In addition, the clovers obtained with ZnTPPS^{4-} (Figure 5b,d) have more angular leaf structures. In

spite of these minor differences, the strong similarities in the dendritic features and basic 4-fold symmetry suggest that they might all share a common molecular packing structure.

Single crystals suitable for X-ray structure determination of the solids that form these cloverlike structures have not yet been obtained. However, XRD measurements of the clovers supported on glass slides or Si wafers (Figure 6) indicate that all of the clovers shown in Figure 5 have similar crystalline structures. Specifically, the reflections from the clovers occur at almost the same angles and have roughly similar line widths. The largest distance (smallest angle) common to all of the clovers is 1.1 nm. On the other hand, the intensities of the reflections vary greatly. It remains to be determined whether each clover is a single crystal despite its complex shape, as is often the case for snowflakes, which also form by a diffusion-limited growth process.

The UV-visible absorption spectrum of the Zn/Sn clovers is shown in Figure 7. The spectrum shows evidence of one or

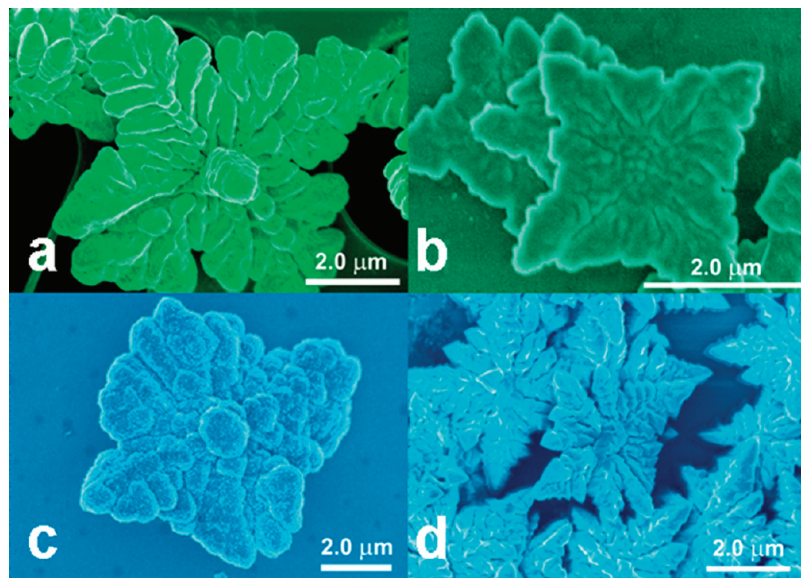


Figure 5. Cloverlike structures obtained from (a) SnTPPS^{4-} and $\text{ZnT}(\text{N-EtOH-4-Py})\text{P}^{4+}$, (b) ZnTPPS^{4-} and $\text{SnT}(\text{N-EtOH-4-Py})\text{P}^{4+}$, (c) SnTPPS^{4-} and $\text{SnT}(\text{N-EtOH-4-Py})\text{P}^{4+}$, and (d) ZnTPPS^{4-} and $\text{ZnT}(\text{N-EtOH-4-Py})\text{P}^{4+}$.

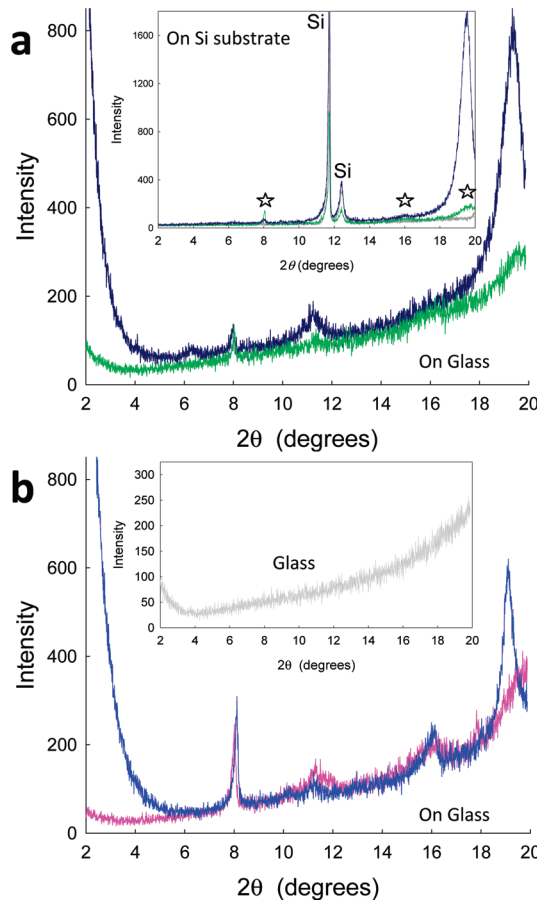


Figure 6. (a) XRD data for Sn/Zn clovers [SnTPPS^{4-} and $\text{ZnT}(\text{N-EtOH-4-Py})\text{P}^{4+}$] (green) and for the Zn/Sn clovers (dark blue) on glass slides. Inset: Sn/Zn (green) and Zn/Sn (dark blue) clovers on the Si wafer and the Si substrate (gray); the stars indicate reflections from the clovers. (b) XRD data for the Zn/Zn clovers (blue) and Sn/Sn clovers (pink) on glass (inset). All samples are dried as follows: Sn/Zn , Sn/Sn , and Zn/Zn by mild heating and Zn/Sn at room temperature.

two J-aggregate bands near 490 nm originating from the Soret transitions, and the long wavelength tail above 620 nm is suggestive of further J-aggregate bands associated with the

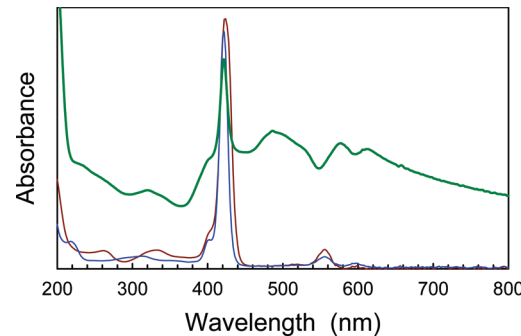


Figure 7. UV-visible absorption spectra of a suspension of the Zn/Sn clovers (green) and the constituent porphyrins ZnTPPS^{4-} (blue) and $\text{SnT}(\text{N-EtOH-4-Py})\text{P}^{4+}$ (red). The J-aggregate band seen near 500 nm for the Zn/Sn clovers is indicative of exciton delocalization over multiple porphyrins.

monomer-like Q bands. Porphyrin J-aggregates typically have molecules in a slipped stacked configuration, and several porphyrins of the same type in the stacks are coupled electronically,³⁵ that is, excitons are delocalized over at least several molecules. To date, attempts to obtain UV-visible spectra of the Sn/Zn clovers have not produced reliable results, probably because their greater thickness relative to the Zn/Sn clovers insures almost complete extinction of visible light. Nevertheless, the similarity of the XRD patterns would suggest that a similar stacking of the porphyrins and exciton delocalization occurs for the Sn/Zn clovers.

Conductive AFM studies were undertaken for the clovers composed of equal proportions of electron donor molecules (Zn porphyrins) and electron acceptor molecules (Sn porphyrins). Figure 8a and Figure S6a of the Supporting Information show AFM images of the Zn/Sn clovers on p-doped conductive Si substrates. The tunneling currents from the surface through the Zn/Sn clovers to a point on the top surface, in the absence and presence of illumination by visible light, are shown in Figure 8b,c. A more than 5-fold increase in current (at -12 V) between the substrate and the tip is observed upon illumination of the

(35) McRae, E. G.; Kasha, M. *J. Chem. Phys.* **1958**, 28, 721.

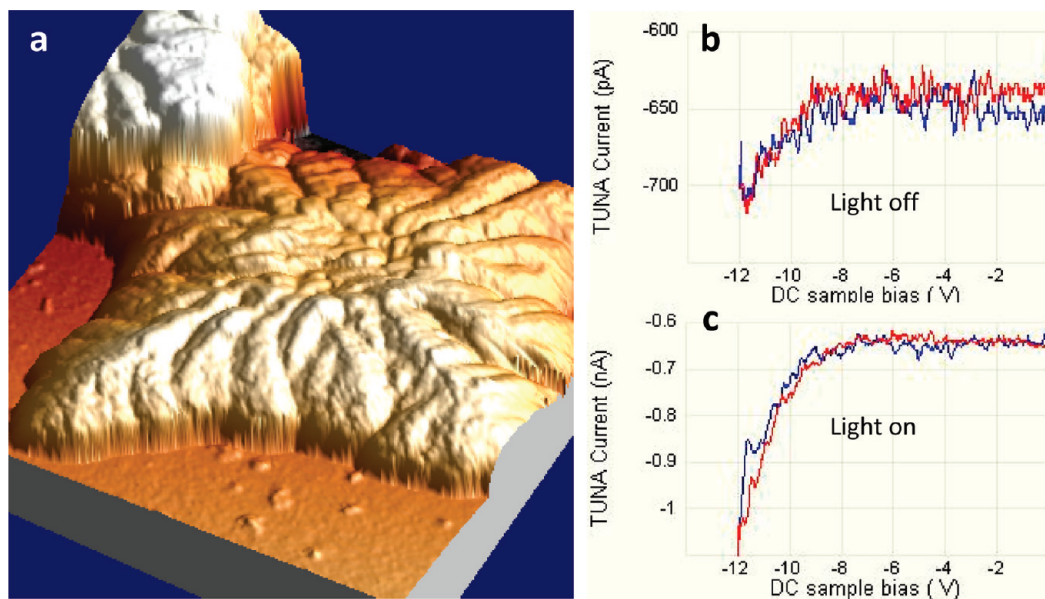


Figure 8. AFM image ($5\text{ }\mu\text{m} \times 5\text{ }\mu\text{m}$) of a ZnTPPS^{4-} and $\text{SnT}(\text{N-EtOH-4-Py})\text{P}^{4+}$ clover (a) and TUNA current–voltage curve for conduction to the AFM Ti/Pt tip at a point on the clover surface through the clover from a p-doped conductive Si substrate with $20\text{ }\Omega\text{ cm}$ resistivity in the dark (b) and when illuminated with the cold incandescent lamp of the AFM instrument (c).

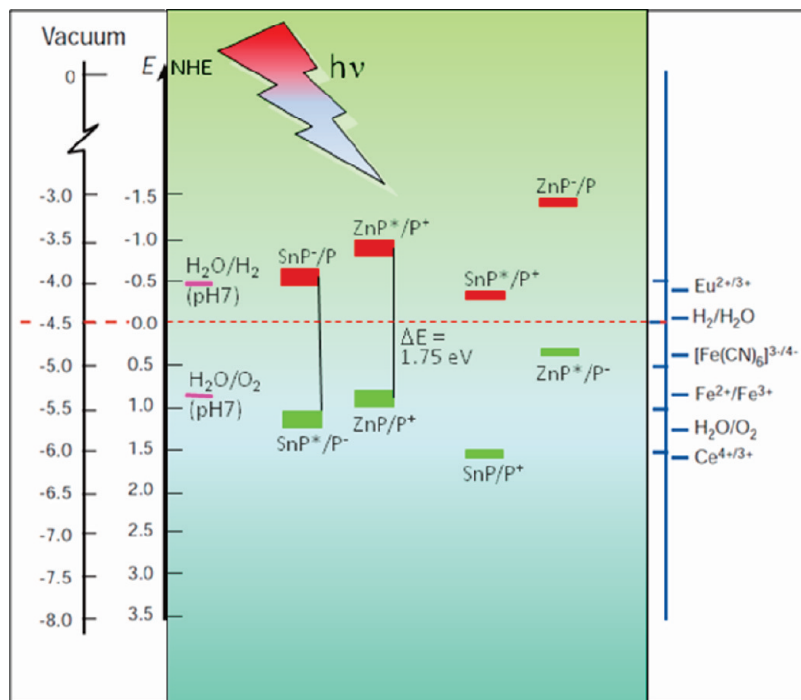


Figure 9. Schematic showing the approximate valence and conduction band energies of Sn(IV) and Zn(II) porphyrins, based on the redox potentials of the metallooctaethylporphyrin ground and lowest excited states.^{37,38} An extended version showing the porphyrin potentials in relation to common inorganic semiconductors is provided in Figure S7 of the Supporting Information.

Zn/Sn clover. Conducting AFM measurements on other Zn/Sn clovers shows similar changes in current upon illumination (see Figure S6b of the Supporting Information) but do not show the increase in dark current seen in Figure 8b that is probably due to stray light from an alignment laser. Remarkably, photoconductivity has not been observed for the Sn/Zn clovers (Figure S6c in the Supporting Information), despite the similarity in the crystal structures indicated by the XRD data.

The photoconductivity of the Zn/Sn clovers can be understood in terms of the energetics of the molecular excitations (charge-

transfer excitons)³⁶ occurring in the illuminated solid. Sn(IV) porphyrins are considered acceptors, and Zn(II) porphyrins are considered donors because of their respective redox potentials (Figure 9 and Figure S7 of the Supporting Information). For both the ground state and the (triplet) excited states, the potentials for related redox processes are almost 1.0 V more negative for Zn(II) than for Sn(IV) porphyrins (based on

(36) Knoester, J.; Agranovich, V. M. In *Electronic Excitations in Organic Based Nanostructures*; Agranovich, V. M., Bassani, G. F., Eds.; Elsevier Academic Press: Amsterdam, 2003; Chapter 1.

published potentials SnOEP and ZnOEP complexes).³⁷ The states connected by solid black lines in Figure 9 indicate those relevant for photoexcitation of the clovers containing Zn and Sn porphyrins. The excited triplet state of the Zn porphyrin has a more negative potential than, and can easily reduce, the Sn porphyrin in either its ground or its excited state. Reduction moves an electron to an adjacent Sn porphyrin and leaves a hole at the Zn porphyrin. The electron (anion) and hole (cation) can then stay bound, but having the hole and electron on different porphyrin molecules increases their separation distance and the probability of free charge-carrier formation. The reduction of the Sn porphyrin in its excited state by the ground-state Zn porphyrin can also occur and leads to a similar charge-separated species.

Another consideration for electron transfer in the clovers is the shift in the energy levels in Figure 9 (shown for SnOEP and ZnOEP)^{37,38} that are present for the porphyrin having the extremely electron-withdrawing pyridinium substituents. [There is a +500 mV shift in the ring reduction potential for T(N-Me-4-Py)P⁴⁺, the methyl analogue of T(N-EtOH-4-Py)P⁴⁺, relative to TPPS⁴⁻.³⁸] For the photoconductive Zn/Sn clovers, the levels shown in Figure 9 should be shifted down an additional 500 mV for SnT(N-EtOH-4-Py)P⁴⁺ because of the effect of the pyridinium substituents. This further enhances the electron acceptor ability of the Sn porphyrin and favors electron transfer. In contrast, for the Sn/Zn clovers, it is the energy levels of the donor ZnT(N-EtOH-4-Py)P⁴⁺ that shift by +500 mV, decreasing the potential difference between the donor and the acceptor and the driving force for electron transfer.

Finally, models of conductivity in classical donor–acceptor solids such as TTF-TCNQ^{39–41} typically invoke the stacking pattern of the molecules:³⁶ A segregated structure (Figure 10a) generally results in conductivity or photoconductivity, whereas interleaved stacking (Figure 10b) usually leads to electrical insulators. Recent resonance Raman studies of binary porphyrin nanotubes¹³ have indicated an internal structure where the two types of porphyrins ($\text{H}_4\text{TPPS}^{2-}$ and $\text{SnTPyP}^{4+/5+}$) are segregated in cylindrical layers.⁴² While further studies are needed to definitively determine the internal stacking arrangement in the clovers, we note that the slipped stacks of $\pi-\pi$ interacting porphyrins, suggested by the optical spectrum in Figure 7, would form four columns of the ionic substituents of the porphyrins, leading to electrostatic π -system channels in the clovers. (These electrostatic channels can be visualized as the pink or blue columns in Figure 10a having either positive or negative charges at the corners of the square prisms representing the porphyrins.) These columns of ions may also affect the photoconductivity. The photoexcitation of the Zn/Sn clovers results in electrons on $\text{SnT}(\text{N-EtOH-4-Py})\text{P}^{4+}$ in columns of positive charges of the pyridinium groups. Conversely, the holes remaining on ZnTPPS^{4-} see channels formed by the negative charges of the sulfonate groups. In contrast, the Sn/Zn clovers, which are not

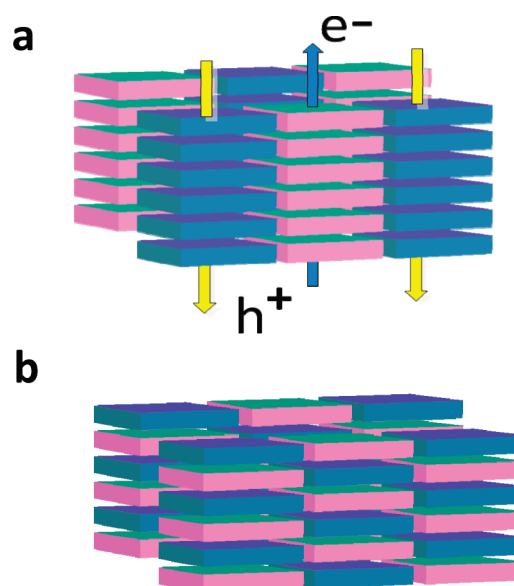


Figure 10. Idealized packing for donor–acceptor solids: (a) segregated stacking and (b) interleaved stacking.³⁶ As drawn, the blocks in panel a would represent H-aggregates, so the stacks must actually be tilted to represent the slipped stacks of J-aggregates. Slipped stacks would still produce the columns of charges at the corners as discussed in the text.

photoconductive (see Figure S6c of the Supporting Information), have the holes on the positively charged porphyrins and the electrons on the negatively charged porphyrins—a condition that may be energetically unfavorable and conducive to electron–hole recombination.

Conclusions

The self-assembled porphyrin structures reported here are unusual not only because of their elaborate dendritic morphologies but also because they provide examples of self-assembled organic materials where the structure is largely independent of the electron donor or acceptor nature of the constituent molecules. This raises the possibility of making binary solids with tunable functional characteristics. To reflect the potential for cooperative interactions between the component porphyrins, we refer to this class of organic materials as *cooperative binary ionic* (CBI) solids. Such materials may be of interest for solar energy and other applications, as they provide new possibilities for varying important photophysical and electronic properties, as well as the possibility of emergent properties. Other CBI materials self-assembled from donor and acceptor porphyrins or other combinations of cooperative functionality (e.g., light-harvesting porphyrins and catalytic porphyrins) have recently been prepared in our laboratories. An example to be reported shortly is the cloverlike structure shown in Figure S5a of the Supporting Information, produced from ZnTPPS^{4-} and $\text{Co}^{\text{III}}\text{T}(\text{N-EtOH-4-Py})\text{P}^{4+}$. This combines a Zn-porphyrin electron donor and a Co-porphyrin catalyst for CO_2 reduction^{43–45} to produce a nanostructure potentially capable of photoassisted CO_2 conversion to CO.

Acknowledgment. Sandia is a multiprogram laboratory operated by Sandia Corporation, a Lockheed Martin Company, for the United

- (37) Davis, D. G. In *The Porphyrins*; Dolphin, D., Ed.; Academic Press: New York, 1978; Vol. V, Chapter 4.
- (38) Kadish, K. M.; Royal, G.; Van Caemelbecke, E.; Gueletti, L. In *The Porphyrin Handbook*; Kadish, K. M., Smith, K. M., Guilard, R., Eds.; Academic Press: San Diego, CA, 2000; Vol. 9, Chapter 59.
- (39) Cavalione, F.; Clementi, E. *J. Chem. Phys.* **1975**, *63*, 4304.
- (40) Alves, H.; Molinari, A. S.; Xie, H.; Morpurgo, A. F. *Nat. Mater.* **2008**, *7*, 574.
- (41) Fraxedas, J. *Molecular Organic Materials: from Molecules to Crystalline Solids*; Cambridge University Press: Cambridge, 2006.
- (42) Franco, R.; Jacobsen, J. L.; Wang, H.; Wang, Z.; Istvan, K.; Schore, N. E.; Medforth, C. J.; Shelnutt, J. A. *Phys. Chem. Chem. Phys.* **2010**, *12*, 4072.

- (43) Furuya, N.; Koide, S. *Electrochim. Acta* **1991**, *36*, 1309.
- (44) Furuya, N.; Matsui, K. *J. Electroanal. Chem.* **1989**, *277*, 181.
- (45) Magdesieva, T. V.; Yamamoto, T.; Tryk, D. A.; Fujishima, A. *J. Electrochim. Soc.* **2002**, *149*, D89.

States Department of Energy's National Nuclear Security Administration under Contract DEAC04-94AL85000.

Supporting Information Available: High magnification SEM images of Sn/Zn clovers, SEM images showing the development of the clovers during growth, SEM images showing morphological diversity for clovers grown at high ionic strengths and high temperatures, SEM image of ZnTPPS/CoT(N-EtOH-4-Py)P

biomorphs, TEM image and MnTPPS/ZnT(N-EtOH-4-Py)P biomorphs, AFM image of Sn/Zn clover and photoconductivity data for Sn/Zn and Zn/Sn clovers, and an extended illustration of the energy levels of Zn and Sn porphyrins and common semiconductors. This material is available free of charge via the Internet at <http://pubs.acs.org>.

JA102194X